

Residual stress distributions in athermally deformed amorphous solids from atomistic simulations

Céline Ruscher and Jörg Rottler

*Department of Physics and Astronomy and Stewart Blusson Quantum Matter Institute,
University of British Columbia, Vancouver BC V6T 1Z1, Canada*

By combining atomistic simulations with the frozen matrix approach, we reveal the evolution of the local residual stress distribution, $P(x)$, in an amorphous packing upon deformation. We find a pseudogap form $P(x) \sim x^\theta$ in the freshly quenched state and in the early stages of deformation. After a few percent strain, however, $P(x)$ starts to develop a plateau p_0 in the small x limit, where $p_0 \sim L^{-p}$ with L the system size. A direct comparison with the system size scaling of the stress drops shows that the statistical properties of avalanches are controlled by θ in the transient regime and the plateau exponent p in the steady state flow.

Upon deformation, amorphous materials such as foams, emulsions, colloidal or metallic glasses behave as solids when the applied shear stress is lower than the yield stress and start to flow above this critical value [1]. The emergence of plasticity is associated with local rearrangements of particles in shear transformation zones (STs) which interact elastically and can organise spatially in transient or permanent shear-bands [2, 4, 5]. Moreover, individual STs can trigger other unstable regions in the glass thus causing collective failure events in the form of avalanches. Intermittent yet steady flow can be maintained where the stress alternates between elastic increases and sudden stress drops which exhibit scale free statistics. Specifically, the avalanche size distribution has the form $P(S, L) \sim S^\tau f(S/S_{\max})$ with the largest avalanches scaling with system size L as $S_{\max} \sim L^{d_f}$. Much attention has been given to understand the scaling properties of $P(S, L)$ and the related universality class to which the yielding transition belongs [6–8].

Important conceptual advance was made in a series of papers by Lin *et al.* [8–11], who pointed out that despite strong similarities, the yielding transition is distinct from the related and well-studied depinning transition. In particular, the authors recognized the importance of the distribution of residual stress $x = \sigma_Y - \sigma$, where σ_Y is the local yield stress of a region and σ the local stress in that region, and argued that it features a pseudogap $\lim_{x \rightarrow 0} P(x) \sim x^\theta$ with $\theta > 0$ in plastic flow. Supported by simulations of mesoscale elastoplastic models (EPM) [12], the authors suggested that the statistics of the weakest sites, i.e. the behavior of $P(x)$ for small x , should determine the statistics of the avalanche size distribution, and obtained a scaling relation $\tau = 2 - \frac{\theta}{\theta+1} \frac{d}{d_f}$ where d is the spatial dimension [8]. This description establishes a firm link between the microscopic statistical properties of the amorphous solid and the macroscopically observed statistical properties of collective yield events, and defines the yielding universality class by the existence of a distinct exponent θ that does not enter the related depinning phenomenon.

However, in two separate and very recent contribu-

tions, Ferrero and Jagla [13] and Tyukodi *et al.* [14] questioned the validity of the pseudogap description. In simulations of steady state flow with EPMS, they reported that $\lim_{x \rightarrow 0} P(x) \sim x^0$, i.e. $P(x)$ is analytic as for the depinning transition when small enough values of x are accessed. While the quantity $P(x)$ is straightforward to extract in EPMS, no direct studies of $P(x)$ exist in particle based models of amorphous solids. In this work, we address by means of atomistic simulations the question of the existence of the pseudogap for a wide range of deformations starting from quenched configurations into the steady-state regime. Using the frozen matrix method [15], we can access residual stresses and determine the distribution $P(x)$. While the description in terms of a pseudogap is valid in the as-quenched state and the early stages of deformation, we find the emergence of a plateau, i.e. $\lim_{x \rightarrow 0} P(x) \sim x^0$ in the late transient and stationary regimes. As observed in the recent EPM works, the scaling behavior for avalanches are determined by the system size scaling of the plateau value of $P(x)$. Although $P(x)$ does develop a pseudogap in the thermodynamic limit, the value of the exponent θ does not enter in the statistical properties of the avalanches.

We consider the 2D binary Lennard-Jones mixture introduced by Lançon *et al.* [1] and widely used to investigate the elastoplastic properties of amorphous solids [2, 3, 17]. We modify it to ensure that the potential is smoothed and shifted at the truncation distance. Details are available in the Supplementary Information (SI). The two types of particles have the same mass of unit m . The units of energy and distance are both given by the interspecies interaction and are respectively ε and σ . Finally the unit of time is $\tau_0 = \sigma \sqrt{m/\varepsilon}$. For this system, the glass transition temperature is $T_g = 0.325\varepsilon/k_B$ where k_B is Boltzmann's constant. Different system sizes $L \in [27, 300]$ have been investigated and at least 5000 independent glassy configurations have been generated per system size. The glass samples are obtained by rapidly cooling initial configurations equilibrated at $T = 2T_g$ at rate $dT/dt = 2 \cdot 10^{-3}$. Simple shear deformations are systematically imposed using the athermal quasistatic shear

(AQS) protocol, where the strain increment is chosen as $\delta\gamma = 5 \cdot 10^{-5}$ and the energy is relaxed through conjugate gradient methods. For this system, the transition to the stationary regime is observed when the strain $\gamma \geq 7\%$.

The frozen matrix method has been used successfully in earlier studies to reveal the spatially heterogeneous (visco)elastic [19, 20] and plastic [17] properties of disordered solids. Following Patinet *et al.* [17], we consider circular regions of size R , in which particles are allowed to relax, embedded in a frozen environment where particles can only move affinely. Therefore, plastic activity can only occur inside the circular region. In the following, we refer to deformations of the whole (periodic) simulation box as *global* and to deformations of the circular regions as *local*.

To detect plastic events, we revisit an energy-based criterion introduced in ref. 5 that suits perfectly the AQS protocol. The observable $\kappa = (U_{aff} - U_0)/(N\delta\gamma^2)$ measures the mismatch between the energy associated with the affine displacement U_{aff} and the inherent structure U_{IS} . As shown in the SI, it is possible to determine analytically a lower bound to κ below which system behaves only elastically. In this work we consider events that have $\kappa \geq 30$ as plastic.

We start by deforming $5 \cdot 10^4$ independent quenched samples of size $L = 100$ and investigating globally the first occurrence of plasticity, which thus measures the distribution of weakest sites x_{min} in the samples. Results are shown in Figure 1(top), where we find that $P(x_{min})$ can be fit with a Weibull distribution [22]. According to extreme value statistics, the underlying distribution of yield stresses should have the form $P(x) \sim x^\theta$ as required by mechanical stability. This is indeed what we can observe in Fig. 1(top) where we measure the exponent $\theta \sim 0.37$.

We then monitor what happens at the local scale by randomly selecting $2 \cdot 10^5$ local regions in the undeformed samples with different values of $R \in [5, 20]$ and straining them up to the first plastic event. The pdf of the residual stresses are also shown in Fig. 1(top), where we observe a power law regime with an exponent θ that depends apparently on R , and the value obtained from $P(x_{min})$ is only recovered in the limit of large R . This effect is directly related to the constraint imposed by the frozen boundary, which prevents nonaffine relaxation outside the circular region and therefore makes the rearrangements more difficult. However, it is interesting to note that for $R \leq 10$, a crossover in the power law appears and for $x < \langle x_{min} \rangle$, one finds $P(x) \sim x^\theta$ with $\theta \approx 0.37$. Even if the small x regime is less than one decade for $R = 5.0$, the frozen matrix method seems to reveal correctly the regime where $x < \langle x_{min} \rangle$, and it is therefore reasonable to probe what happens when we start deforming the configurations.

The hypothesis of a pseudogap form of $P(x) \sim x^\theta$ combined with the idea of independence of plastic events

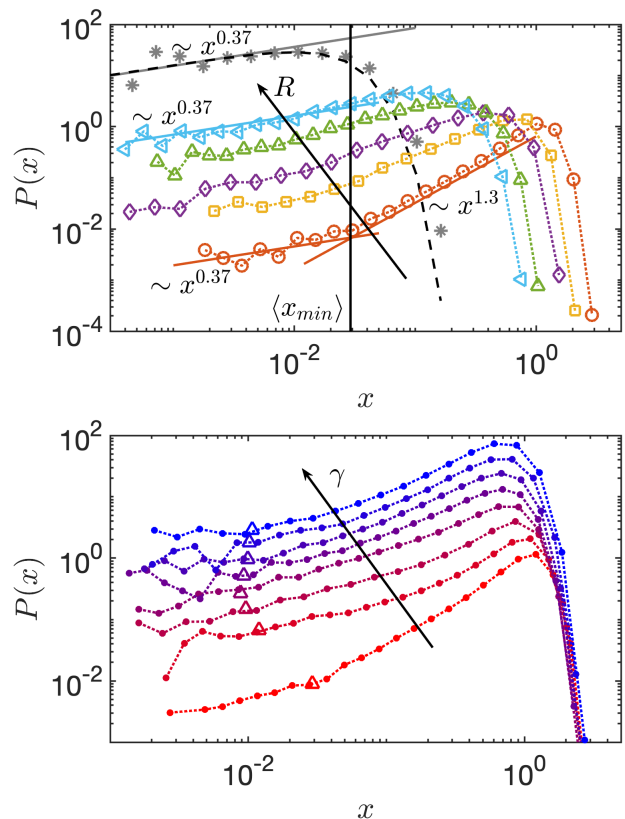


FIG. 1. Top: Distribution of residual stresses $P(x)$ for circular regions of size $R = 5.0(\circ)$, $R = 7.5(\square)$, $R = 10.0(\diamond)$, $R = 15.0(\triangle)$, $R = 20.00(\nabla)$. The circular regions are all extracted from global configurations of size $L = 100$ for which the distribution of weakest site $P(x_{min})(*)$ is also shown. The dashed line corresponds to the Weibull fit with parameters $k = 1.37, \lambda = 0.026$. The vertical solid line indicates the value of $\langle x_{min} \rangle$. Bottom: Evolution of $P(x)$ upon deformation obtained for $R = 5.0$. Curves have been shifted for sake of clarity. Values of the strain are $\gamma = \{0, 0.01, 0.02, 0.04, 0.06, 0.08, 0.12, 0.18\}$. The triangles indicate the value of $\langle x_{min} \rangle$ for each strain.

implies on the one hand that the distribution of weakest sites behaves as $P(x_{min}) \sim x_{min}^\theta$, and on the other hand a scaling relation between $\langle x_{min} \rangle$ and the system size, $\langle x_{min} \rangle \sim L^{-\alpha}$ where $\alpha = d/(1 + \theta)$ [9, 22]. However, both atomistic simulations [22, 23] and EPMS [9] indicate that once strained configurations are considered, the pdf of weakest sites changes drastically and $P(x_{min}) \sim x_{min}^0$. On the other hand, EPM simulations suggest that the scaling relation $\langle x_{min} \rangle \sim L^{-\alpha}$ is still preserved [9]. Nonetheless, as pointed out by Ferrero and Jagla [13], there is often a mismatch between θ obtained from scaling relation on $\langle x_{min} \rangle$ and θ inferred from $P(x)$. So how to understand this apparent discrepancy?

Inspection of Fig. 1(bottom) reveals that for the present samples, the pseudogap description remains valid during the first stages of deformation. We still observe a

crossover between $P(x) \sim x^\theta$ for $x < \langle x_{min} \rangle$ and another power law regime for larger x . However, this crossover becomes less and less pronounced upon increasing deformation, and the value of the power law exponent for the regime where $x > \langle x_{min} \rangle$ decreases with respect to the freshly quenched state. This flattening behavior has also been observed in EPM simulations [10, 24]. However, after only $\sim 6\%$ strain, we observe the emergence of a plateau for $x < \langle x_{min} \rangle$. The strain at which the plateau appears to depend on L as observed in Fig. 2 (top) for two values of the strain. Indeed we find for example that for $L = 53$, the departure occurs at $\sim 4\%$ strain but at $\sim 8\%$ strain for $L = 200$ (see Fig S5).

This scenario reveals that once we start to deform the material, more and more sites are driven towards their instability threshold, and when the strain approaches the critical stress, there remains a fraction of sites on the verge of failure. Lin *et al.* attributed the existence of the pseudogap to the alternating sign in the Eshelby-like stress propagator of STs [8]. In the case of depinning, by contrast, the interaction is always positive, thus leading to $P(x) \sim x^0$. Here from the moment configurations are being deformed, the elastic long-range interactions are going to bring more and more sites towards instability. The most unstable sites are going to be more sensitive to the destabilizing part of the kernel and therefore, for very small residual stresses, the situation resembles the depinning transition. As deformation progresses, the above arguments would suggest a deepening pseudogap regime because of the alternating sign of the elastic interactions [11]. This is indeed what we observe in the regime where $x > \langle x_{min} \rangle$, as the flattening observed right after deforming the as-quenched configurations is followed by a deepening at larger strains.

In Fig. 2 we analyse the system size dependence of the emergence of the plateau. As mentioned above, we observe in both transient and stationary regimes, the appearance of a plateau in $P(x)$ and the smaller the system, the sooner the departure from the power law regime characterized by an exponent that we denote $\tilde{\theta}$ to make a distinction with θ associated with the pseudogap description. As already reported for EPMs [13, 14], a scaling relation exists for the height of the plateau $p_0 \sim L^{-p}$ and for the crossover value of the stress for which the pdf departs from the power law regime, $x_c \sim L^{-p/\tilde{\theta}}$. It is therefore possible to rescale $P(x)$ as suggested in the bottom panel of Fig. 2, where we have represented $P(x)L^p$ as a function of $xL^{p/\tilde{\theta}}$. We find $p \approx 0.65$ (resp. $p \approx 0.75$) and $\tilde{\theta} \approx 1.05$ (resp. $\tilde{\theta} \approx 0.75$) for the stationary regime (resp. transient regime). We notice that the values of p and $\tilde{\theta}$ in the stationary regime are slightly larger than the values $p \approx 0.55 - 0.60$ and $\tilde{\theta} \approx 0.66 - 0.75$ found with EPMs [13, 14]. This difference could be possibly related to our use of the frozen matrix approach. We also observe that for both transient and steady-state regimes, the average

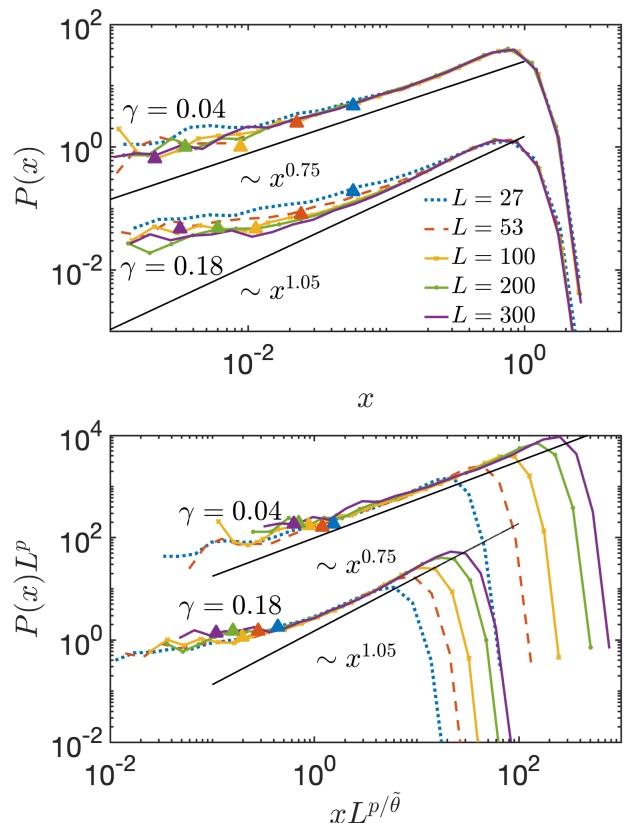


FIG. 2. (Top) Unscaled probability distribution function of the residual stresses for different system sizes in the transient regime $\gamma = 0.04$ and stationary regime $\gamma = 0.18$ where $\tilde{\theta} = 0.75$ and $\tilde{\theta} = 1.05$ (see text) respectively. The curves of $P(x)$ associated with the transient regime have been shifted by a factor 30. (Bottom) Scaled probability distribution function of the residual stresses. The exponent $p = 0.75$ and $p = 0.65$ in the transient and stationary regimes respectively. In both panels, the triangles indicate for each system size the position of $\langle x_{min} \rangle$.

positions of $\langle x_{min} \rangle$ fall either onto the plateau or in the crossover region suggesting that the power law observed for $x > \langle x_{min} \rangle$ does not determine the small stress limit.

Extreme value statistics allows us to determine a scaling relation for $\langle x_{min} \rangle$. Indeed one has $\int_0^{\langle x_{min} \rangle} P(x) dx \sim 1/L^d$. For small deformation, the pseudogap is valid and therefore $P(x) \sim x^\theta$ which leads to $\langle x_{min} \rangle \sim L^{-\alpha}$ with $\alpha = d/(1 + \theta)$. For large deformation, the small stress limit can be described by $P(x) = p_0$ and if one assumes that $p_0 \sim L^{-p}$ we find $\langle x_{min} \rangle \sim L^{-\alpha}$ where $\alpha = d - p$.

This system size scaling of the weakest sites can be compared to the avalanche statistics. As in ref. 25 we define the avalanche size as $S = L^d \Delta\sigma$ where $\Delta\sigma$ corresponds to the size of the stress drop. It is known that the average stress drops scale as $\langle \Delta\sigma \rangle = \langle S \rangle / L^d \sim L^{-\alpha_S}$. We therefore measure $\langle S \rangle$ upon deformation for the different system sizes and obtain $\alpha_S / \tilde{\theta}$ from the system size

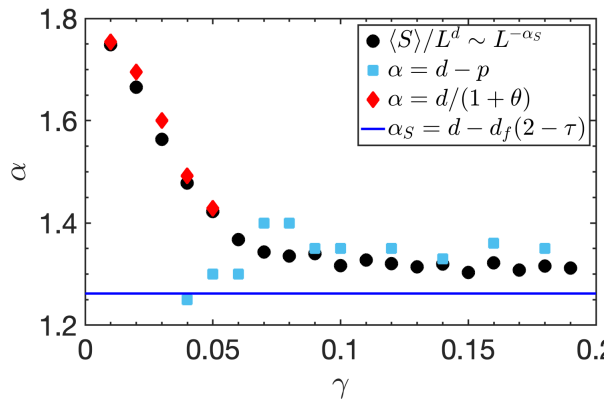


FIG. 3. Evolution of the α exponent upon deformation computed from four different relations. See text for details.

scaling. We observe in Fig. 3 that α_S is decreasing upon deformation and reaches a final value of ≈ 1.31 in the stationary regime. In this latter regime, we find good agreement between α_S and $\alpha = d - p$. In the stationary regime, $P(x) \sim L^{-p}$ and the plasticity is governed by the plateau exponent p . In the late transient regime, the agreement is less good for $\gamma \leq 0.05$ suggesting that p is no more the key parameter. We have already noticed that for these values of the strain, there is not necessarily a plateau for the largest L as shown in Fig. 2 (top). This suggests that the behavior of $P(x)$ is intermediate in the small x limit in this range of strains. One can therefore extract θ in the regime $x < \langle x_{min} \rangle$ and use its value to determine α . Even if the fitting range is limited (see SI for details), we find good agreement with α_S . For $\gamma \leq 0.05$, the scaling properties of stress drops are therefore controlled by the exponent θ .

We also determined the distribution of avalanche sizes $P(S, L)$ and its scaling behavior in Fig. 4. In the transient regime ($\gamma = 0.04$), our distributions have not yet developed a clear power law regime and a reliable extraction of the avalanche size exponent τ is not possible. In the stationary regime ($\gamma = 0.18$), the larger system sizes develop a clear power law region centered on the value of $\langle S \rangle$, and we find $\tau \approx 1.10$ and $d_f \approx 0.82$. The fractal dimension appears to change upon deformation as we find $d_f \approx 0.75$ when $\gamma = 0.04$. These values are smaller than $\tau \approx 1.25$ and $d_f \approx 0.9$ reported in previous steady state 2D MD simulations using slightly different particle models and deformation protocols [7, 26]. By equating the average stress drops computed directly and by integrating over the assumed power law form of $P(S, L)$, one can derive the relation $\alpha_S = d - d_f(2 - \tau)$, which yields $\alpha_S \approx 1.26$ for our measured values of τ and d_f at $\gamma = 0.18$. This value lies slightly below the value of $\alpha_S \approx 1.31$ from direct measurement of the system size scaling of $\langle \Delta\sigma \rangle$. The average $\langle \Delta\sigma \rangle$ is dominated by large

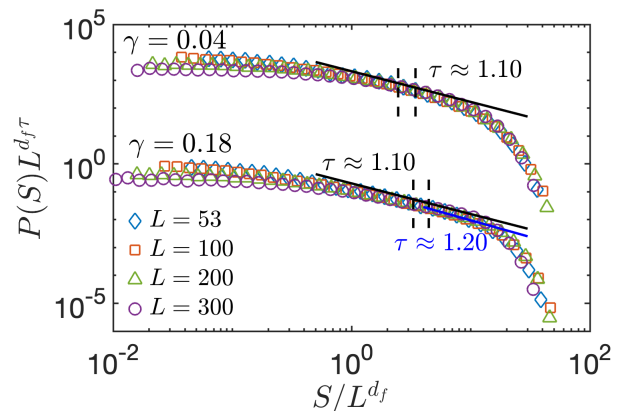


FIG. 4. Scaled distribution of avalanches $P(S, L)$ in the transient regime $\gamma = 0.04$ and in the stationary regime $\gamma = 0.18$. The distribution in the transient regime has been shifted by a factor 10000. The fractal dimension $d_f \approx 0.82$ and the avalanche exponent $\tau \approx 1.1$. The vertical dashed lines correspond to the location of $\langle S \rangle$ for $L = 53$ and $L = 300$.

avalanches, while $P(S)$ reflects all the possible size of plastic events. Indeed if we look at the position of $\langle S \rangle$ on $P(S)$ we realise that most of the fitted power law corresponds to small stress drops. Despite the small range of S available to us in the atomistic systems, one can attempt to extract τ for $S \geq \langle S \rangle$, and one finds $\tau \approx 1.2$ as shown in Figure 4. This higher value of τ would yield $\alpha_S \approx 1.34$ which is in better agreement with the value from the mean sizes of the stress drops.

Summarizing, a direct determination of the distribution $P(x)$ of residual stresses $x = \sigma_Y - \sigma$ in atomistic simulations of athermally quasistatically deformed amorphous solids indicates (in agreement with earlier studies at the EPM level) that $P(x)$ crosses over from $P(x) \sim x^\theta$ to nonsingular behavior upon plastic deformation. In our model system the crossover occurs at a few percent deformation, but the precise location is almost certainly preparation dependent. Interestingly, the EPM simulations of Budrikis et al. [24] had reported the formation of a plateau in $P(x)$ already in the transient regime where the stress is much below the critical stress, but concluded that a pseudogap still emerges at the critical stress.

From the scaling of the plateau $p_0 \sim L^{-p}$ one must conclude that for $L \rightarrow \infty$, $P(x)$ does indeed become nonanalytic again. However, the associated exponent θ does not enter the scaling properties of the avalanches as $\langle x_{min} \rangle$ simultaneously decreases with system size and always remains dominated by small values of x in the plateau region [13]. A possible origin of the emergence of this plateau could lie in the tendency of amorphous solids to form transient micro shear bands, in which weak zones tend to accumulate. The one-dimensional character of such zones would make failure more likely along a preferential direction, thus (partially) negating the ef-

fect of the alternating sign in the elastic interaction and leading to more depinning like behavior. A systematic investigation of this connection should be the next step in the development of a statistical theory of amorphous plasticity.

We thank M. Müller, K. Samwer, P. Sollich, and A. Zaccone for interesting discussions of this work. Computing resources were provided by ComputeCanada.

-
- [1] D. Bonn, M. M. Denn, L. Berthier, T. Divoux, and S. Manneville, *Rev. Mod. Phys.* **89**, 035005 (2017).
- [2] A. Argon, *Acta Metallurgica* **27**, 47 (1979).
- [2] M. L. Falk and J. S. Langer, *Phys. Rev. E* **57**, 7192 (1998).
- [4] A. Tanguy, F. Leonforte, and J. L. Barrat, *The European Physical Journal E* **20**, 355 (2006).
- [5] P. Schall, D. A. Weitz, and F. Spaepen, *Science* **318**, 1895 (2007).
- [6] M. Talamali, V. Petäjä, D. Vandembroucq, and S. Roux, *Phys. Rev. E* **84**, 016115 (2011).
- [7] K. M. Salerno and M. O. Robbins, *Phys. Rev. E* **88**, 062206 (2013).
- [8] J. Lin, E. Lerner, A. Rosso, and M. Wyart, *Proceedings of the National Academy of Sciences* **111**, 14382 (2014).
- [9] J. Lin, A. Saade, E. Lerner, A. Rosso, and M. Wyart, *EPL (Europhysics Letters)* **105**, 26003 (2014).
- [10] J. Lin, T. Gueudré, A. Rosso, and M. Wyart, *Phys. Rev. Lett.* **115**, 168001 (2015).
- [11] J. Lin and M. Wyart, *Phys. Rev. X* **6**, 011005 (2016).
- [12] A. Nicolas, E. E. Ferrero, K. Martens, and J.-L. Barrat, *Reviews of Modern Physics* **90**, 045006 (2018).
- [13] E. E. Ferrero and E. A. Jagla, arXiv e-prints, arXiv:1905.05610 (2019), arXiv:1905.05610 [cond-mat.dis-nn].
- [14] B. Tyukodi, D. Vandembroucq, and C. E. Maloney, arXiv e-prints, arXiv:1905.07388 (2019), arXiv:1905.07388 [cond-mat.soft].
- [15] P. Sollich, CECAM meeting (2011).
- [1] F. Lançon and L. Billard, *J. Phys. France* **49**, 249 (1988).
- [17] S. Patinet, D. Vandembroucq, and M. L. Falk, *Phys. Rev. Lett.* **117**, 045501 (2016).
- [3] A. Barbot, M. Lerbinger, A. Hernandez-Garcia, R. García-García, M. L. Falk, D. Vandembroucq, and S. Patinet, *Phys. Rev. E* **97**, 033001 (2018).
- [19] H. Mizuno, S. Mossa, and J.-L. Barrat, *Phys. Rev. E* **87**, 042306 (2013).
- [20] B. Shang, J. Rottler, P. Guan, and J.-L. Barrat, *Physical review letters* **122**, 105501 (2019).
- [5] E. Lerner and I. Procaccia, *Phys. Rev. E* **79**, 066109 (2009).
- [22] S. Karmakar, E. Lerner, and I. Procaccia, *Phys. Rev. E* **82**, 055103(R) (2010).
- [23] H.G.E. Hentschel, P. K. Jaiswal, I. Procaccia, and S. Sastri, *Physical Review E* **92**, 062302 (2015).
- [24] Z. Budrikis, D. F. Castellanos, S. Sandfeld, M. Zaiser, and S. Zapperi, *Nature communications* **8**, 15928 (2017).
- [25] M. Ozawa, L. Berthier, G. Biroli, A. Rosso, and G. Tarjus, *Proceedings of the National Academy of Sciences* **115**, 6656 (2018).
- [26] C. Liu, E. E. Ferrero, F. Puosi, J.-L. Barrat, and K. Martens, *Phys. Rev. Lett.* **116**, 065501 (2016).

Supplementary Information

SIMULATIONS DETAILS

We consider a 2D Lennard-Jones (LJ) binary mixture which has been introduced by Lançon *et al.* [1] to investigate the properties of 2D quasicrystals, and has been shown to be a good glass-former. Following refs. 2 and 3, the N_L large and N_S small particles interact through the potential:

$$V_{ab}(r) = \begin{cases} 4\varepsilon_{ab} \left[\left(\frac{\sigma_{ab}}{r} \right)^{12} - \left(\frac{\sigma_{ab}}{r} \right)^6 \right] + V_S, & \forall r \leq r_{in} \\ \sum_{k=0}^4 C_k r^k & \forall r_{in} < r \leq r_{cut} \\ 0, & \forall r > r_{cut} \end{cases} \quad (1)$$

where $\{a, b\} = \{L, S\}$ and r is the distance between two particles. The potential is shifted at the cutoff distance $r_{cut} = 2.5\sigma_{LS}$ and smoothed for $r_{in} < r \leq r_{cut}$ where $r_{in} = 2.0\sigma_{LS}$ in order to ensure that $V_{ab}(r)$ is twice differentiable. The shift in energy V_S and the coefficients C_k are:

$$\begin{aligned} V_S &= C_0 - 4\varepsilon_{ab} \left[\left(\frac{\sigma_{ab}}{r_{in}} \right)^{12} - \left(\frac{\sigma_{ab}}{r_{in}} \right)^6 \right] \\ C_0 &= -(r_{cut} - r_{in})[3C_1 + C_2(r_{cut} - r_{in})]/6 \\ C_1 &= 24\varepsilon_{ab}\sigma_{ab}^6(r_{in}^6 - 2\sigma^6)/r_{in}^{13} \\ C_2 &= -12\varepsilon_{ab}\sigma_{ab}^6(7r_{in}^6 - 26\sigma^6)/r_{in}^{14} \\ C_3 &= -[3C_1 + 4C_2(r_{cut} - r_{in})]/[3(r_{cut} - r_{in})^2] \\ C_4 &= [C_1 + C_2(r_{cut} - r_{in})]/[3(r_{cut} - r_{in})^3] \end{aligned} \quad (2)$$

The different LJ parameters are $\sigma_{LL} = 2\sin(\pi/5)$, $\sigma_{LS} = 1$, $\sigma_{SS} = 2\sin(\pi/10)$, $\varepsilon_{LL} = \varepsilon_{SS} = 0.5$, $\varepsilon_{SL} = 1$, and all masses are set to $m = 1$. The ratio between large and small particles is chosen such as $N_L/N_S = (1 + \sqrt{5})/4$, and we work at constant density $N/V = 1.0206$.

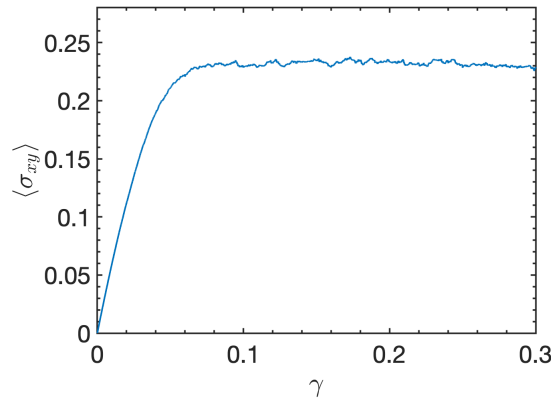


FIG. S1. Average stress $\langle \sigma_{xy} \rangle$ as a function of the applied strain γ for $L = 100$.

All simulations have been carried out using the LAMMPS software [4]. We consider a 2D triclinic simulation box of size L under periodic boundary conditions. To generate the different glass configurations, we first equilibrate systems in the liquid phase at $T = 0.65$ using the Langevin thermostat with a damping parameter $T_{damp} = 1.0$. The timestep is chosen as $\delta t = 0.005$. After equilibration, the different configurations are cooled down to $T = 0$ at $dT/dt = 2 \cdot 10^{-3}$. The deformations are imposed by tilting the simulation box in the x direction by an amount $\delta\gamma_{xy}L$, where $\delta\gamma_{xy} = 5 \cdot 10^{-5}$ is the strain increment. The average stress-strain curve obtained with this protocol is shown in Figure S1. As can be seen, a steady state is established once the strain exceeds 7-8%.

DETERMINATION OF PLASTIC EVENTS

To determine plastic events, we revisit a criterion proposed by Lerner and Procaccia [5], which relies on the difference in potential energy between the affine deformation U_{aff} and the underlying inherent structure U_0 :

$$\kappa = \frac{U_{aff} - U_0}{N\delta\gamma^2} \quad (3)$$

where $\delta\gamma$ is the strain increment. While in ref. 5 a reasonable but arbitrary value of κ was selected, we demonstrate here that there exists a range of κ associated with purely elastic deformation and therefore a lower bound above which κ captures plastic events only.

The following demonstration relies on the hypothesis that we work in the elastic regime, where we first notice that U_{aff} corresponds exactly to the affine (Born) energy only for the first strain increment ($n = 1$) in the AQS protocol. Only when $n \geq 2$, U_{aff} starts to differ from the Born energy due to the relaxation of particles to new energy minima. For a system after n strain increments, the affine strain energy density associated with the affine deformation in the AQS protocol is given by:

$$\rho\phi_{aff,AQS}^{(n)} = \rho\phi^{(n-1)} + \sigma^{(n-1)}\delta\gamma + \frac{G_{aff,AQS}^{(n-1)}}{2}(\delta\gamma)^2 \quad (4)$$

where $\phi^{(n-1)}$ and $\sigma^{(n-1)}$ are respectively the strain energy and the stress of the system after the $(n-1)$ th AQS step, $G_{aff,AQS}^{(n-1)}$ is the value of the shear modulus associated with the affine transformation in the AQS protocol at step n . When $n = 1$ (first deformation), we find

$$\rho\phi_{aff,AQS}^{(1)} = \rho\phi^{(0)} + \sigma^{(0)}\delta\gamma + \frac{G_{aff,AQS}^{(0)}}{2}(\delta\gamma)^2 \quad (5)$$

where in this case $G_{aff,AQS}^{(0)} = G_B$ is the Born shear modulus. The strain energy after relaxation of the potential energy is given by

$$\rho\phi^{(n)} = \rho\phi^{(n-1)} + \sigma^{(n-1)}\delta\gamma + \frac{G}{2}(\delta\gamma)^2 \quad (6)$$

Therefore, considering the difference $(U_{aff} - U_0)/N$ which corresponds to $\phi_{aff,AQS} - \phi^{(n)}$, we find

$$\phi_{aff,AQS} - \phi^{(n)} = \frac{G_{aff,AQS}^{(n-1)} - G}{2\rho}(\delta\gamma)^2 \quad (7)$$

Finally, we can estimate an upper bound for κ in the elastic regime:

$$\kappa = \frac{G_{aff,AQS}^{(n-1)} - G}{2\rho} \leq \frac{G_B - G}{2\rho} \leq \frac{G_B}{2\rho} \quad (8)$$

We determine that $G_B \approx 26$, meaning that the lower bound for plastic activity is $\kappa \approx 13$. To verify our analytical description, we computed κ for each strain increment $\delta\gamma = 5 \cdot 10^{-5}$ upon deformation (up to 30%). Its probability distribution function is shown in Figure S2, where we observe that the distribution is peaked around $\kappa \approx 8$ and a long tail persists for larger value of κ . The peak is associated with elastic contributions. Indeed we measured that $G \approx 12$ for this system so κ is more likely to be $(26 - 12)/2 \approx 7$.

We decided to chose $\kappa \approx 30$ as criterion to ensure to have only plastic contributions. In Figure S3, we observe that κ is matching with stress release in the stationary regime but more interestingly, as suggested in the inset, this criterion allows one to determine plastic events for which no stress drop is measured. This is due to the higher sensitivity of the potential energy to structural rearrangement. The detection in terms of stress drops is constrained by the choice of the strain increment as a stress release would have been certainly noticed with a smaller $\delta\gamma_{xy}$ but this would also imply longer simulation times. Therefore, κ is an efficient criterion to monitor plasticity while working with a finite value of $\delta\gamma_{xy}$.

We also checked that the results are not sensitive to the choice of κ and in particular the value of the exponent θ obtained from the Weibull fit

$$P(x_{min}) = \frac{k}{\lambda} \left(\frac{x_{min}}{\lambda} \right)^{k-1} e^{-(x_{min}/\lambda)^k} \quad (9)$$

where $k = 1 + \theta$, is robust. Results are shown in Figure S4, where we see that for $20 < \kappa < 1000$, θ is roughly constant and ≈ 0.35 .

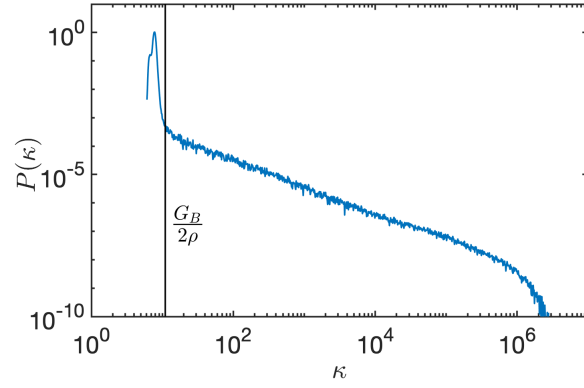


FIG. S2. Probability distribution function of κ where κ has been computed for each strain increment $\delta\gamma$. The vertical solid line represents the lower bound of κ to detect plastic events.

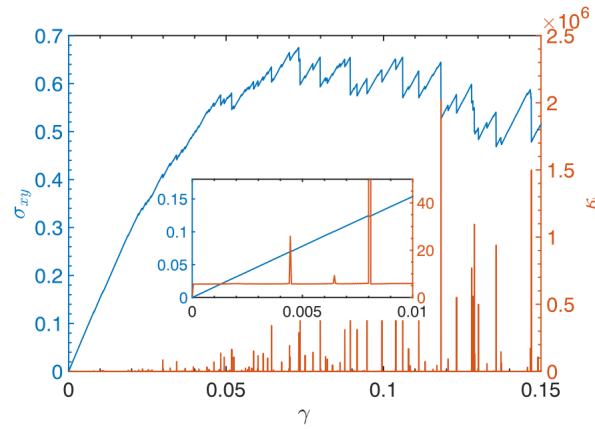


FIG. S3. Main panel: Typical stress-strain curve obtained during the deformation of a global system where $L = 100$. The peaks in the κ observable indicate stress drops. Inset: Zoom in the initial stage of the deformation.

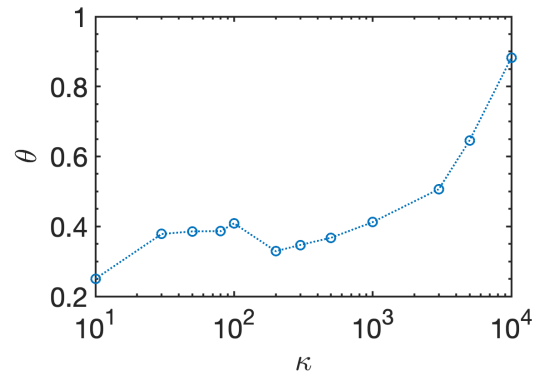


FIG. S4. Evolution of θ with κ computed from Weibull fits on $P(x_{min})$ for global systems of size $L=100$.

EVOLUTION OF $P(x)$ FOR DIFFERENT SIZES

As mentioned in the Letter, the transition from a pseudogap description $P(x) \sim x^\theta$ to $P(x) \sim x^0$ depends on the system size. In Figure S5 we show the evolution of $P(x)$ for $L = 53$ and $L = 200$. We observe that the departure from the power law regime occurs $\approx 4\%$ deformation when $L = 53$ while we have to deform the system up to $\approx 8\%$ to see this behavior for $L = 200$.

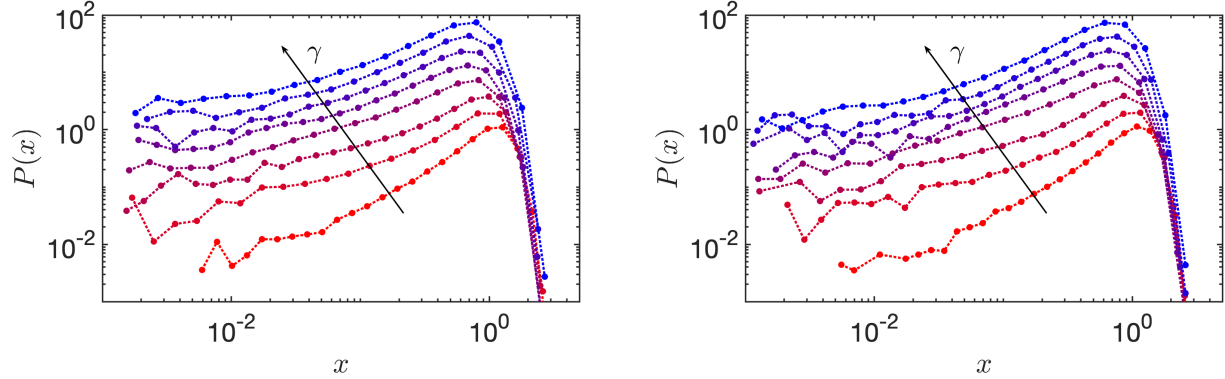


FIG. S5. Distribution of the residual stresses for the small strains obtained for circular region of size $R = 5.0$ taken from system of size $L = 53$ (Left) and $L = 200$ (Right). Values of the strain are $\gamma = \{0, 0.01, 0.02, 0.04, 0.06, 0.08, 0.12, 0.18\}$.

DETERMINATION OF PSEUDOGAP EXPONENT IN THE TRANSIENT REGIME

In the early stage of the deformation, the pseudogap description $P(x) \sim x^\theta$ applies. As shown in Figure S6, two power law regimes are visible. As the weakest sites control the plasticity, we conclude that the relevant value of θ is in the range where $x = \mathcal{O}(\langle x_{min} \rangle)$ as shown in Figure S6.

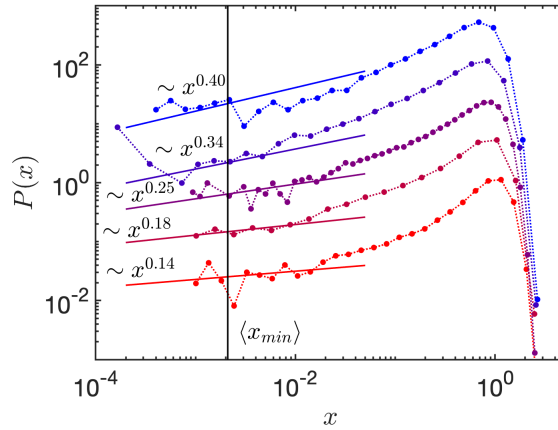


FIG. S6. Distribution of the residual stresses for the small strains obtained for circular region of size $R = 5.0$ taken from system of size $L = 300$. Values of the applied strains are from bottom to top $\gamma = \{0.01, 0.02, 0.03, 0.04, 0.05\}$.

-
- [1] F. Lançon and L. Billard, J. Phys. France **49**, 249 (1988).
 [2] M. L. Falk and J. S. Langer, Phys. Rev. E **57**, 7192 (1998).

- [3] A. Barbot, M. Lerbinger, A. Hernandez-Garcia, R. García-García, M. L. Falk, D. Vandembroucq, and S. Patinet, Phys. Rev. E **97**, 033001 (2018).
- [4] S. J. Plimpton, J Comp Phys **117** (1995).
- [5] E. Lerner and I. Procaccia, Phys. Rev. E **79**, 066109 (2009).